

Supplementary Information for:

**Fabrication of Polymer Nanotubes Containing Nanoparticles and Inside Functionalization**

Kyung Jin Lee, Sa Hoon Min, Hyuntaek Oh and Jyongsik Jang\*

World Class University (WCU) program of Chemical Convergence for Energy & Environment (C<sub>2</sub>E<sub>2</sub>),  
School of Chemical and Biological Engineering, Seoul National University, 599 Gwanangro, Gwanak-gu,  
Seoul 151-742, Korea.

[\*] E-mail: [jsjang@plaza.snu.ac.kr](mailto:jsjang@plaza.snu.ac.kr)

Tel.: +82-2-880-7069

Fax: +82-2-888-1604

## 1. Experimental details

**Materials:** Pluronic block copolymer (F127, P123, P103, P84, and P65) was supplied by BASF and used without purification. All other reagent including ferric chloride, pyrrole, and pyrrole 3-carboxylic acid were purchased from Aldrich. The N-amino pyrrole was obtained from Tokyo Chemical Industry. FITC-Streptavidin, biotin, EDC, and NHS were also ordered from Aldrich and dispersed in 0.1 M of PBS.

**AAO membrane:** AAO membrane which contains perpendicularly aligned cylindrical pore with average pore diameter of 150 nm and length of 60  $\mu\text{m}$  is purchased from Whatman Co.. Well-designed cylindrical pore provides great advantages to generate one dimensional nanomaterials composed of polymeric, metallic, inorganic and carbonic materials. Combining with our VDP process, nanotubular structure with inner hollow and open-end can be readily prepared as reported in our previous works (ref 9, 10 and ref S1).

Ref S1) K. J. Lee, J. H. Oh, Y. Kim, and J. Jang, *Adv. Mater.*, 2006, **18**, 2216; K. J. Lee, J. H. Oh, Y. Kim, and J. Jang, *Chem. Mater.*, 2006, **18**, 5002.

**Fabrication of NPNT and functionalized NPNT in the pore of AAO membrane:** The AAO membrane was soaked into the surfactant solution for 5 min. Typically, the surfactant solution was composed of 1 g of block copolymer, 0.1 g of  $\text{FeCl}_3$ , 2 g of water and 5 g of ethanol. The membrane was moved into the closed vessel and annealed in 80  $^\circ\text{C}$  for 2 min. 2 mmol of pyrrole monomer was added into the reaction vessel per 13 mm of AAO membrane, and VDP was carried out for 2 h. In order to obtain functionalized PPy NPNT membrane, the reaction vessel was evacuated until the inner vacuum pressure reached to  $10^{-2}$  torr, after pyrrole polymerization. Then, 0.5 mmol of COOH and  $\text{NH}_2$  pyrrole was introduced in the reactor per each AAO membrane. Graft polymerization was performed at 150  $^\circ\text{C}$  for 1 h. For PPy nanotubes as a control experiment, AAO template was soaked in ferric chloride aqueous solution (0.2 M) and moved into the reaction chamber with sealing apparatus. The reaction chamber was evacuated to  $10^{-1}$  Torr and 0.1 ml of pyrrole monomer was introduced into chamber. VDP was performed at 80  $^\circ\text{C}$  for 2 h.

**Immobilization of Streptavidin onto COOH-NPNT (Route 1):** The prepared COOH-NPNT membrane was washed with PBS by several times through cartridge method as illustrated in Scheme 2a). 0.4 ml of EDC (10 mM) and NHS (10 mM) solution in PBS was permeated into the COOH-NPNT membrane. The 0.1 ml of FITC-Streptavidin/PBS (1 mg/mL) was reacted, and the AAO membrane was washed again with the 0.1 M of PBS.

**Conjugation of Streptavidin onto biotinlated  $\text{NH}_2$ -NPNT (Route 2):** The  $\text{NH}_2$ -NPNT membrane was also treated by PBS, as same above. The solution composed of 0.2 ml of 10 mM EDC, 0.2 ml of 10 mM NHS,

and 0.1 ml of biotin in PBS (1 mg/ml) was firstly permeated through the NH<sub>2</sub>-NPNT membrane. After then, 0.1 ml of FITC-Streptavidin/PBS (1 mg/mL) was introduced into the cartridge.

**Characterization:** TEM images were taken using JEOL JEM-200CX at an acceleration voltage of 200 kV. The AAO with PPy NPNT was treated by HCl (3M) aqueous solution, and excess amount of absolute ethanol was added. The final products were precipitated and upper solution was removed. The product solution was dropped on the copper grid covered by carbon film. Scanning electron microscopy was obtained with a JEOL 6700 at an acceleration voltage of 10 kV. For the SEM analysis, the products were dropped onto the carbon film and dried. FTIR spectra were recorded on Bomem MB100 spectroscope at a resolution of 4 cm<sup>-1</sup>. The FT-IR spectra were obtained by KBr pellet method with the PPy NPNT precipitated and dried in vacuum oven. Permeable rates of each NPNT membrane were determined with the passing amount of water through the membrane divided by required time. The values displayed in Figure 2 are relative rate with respect to the permeable rate of empty AAO (control). CLSM images were obtained with a Carl Zeiss-LSM510 confocal laser scanning microscope. The CLSM images were observed from the membrane treated by FITC-Streptavidin, without etching of AAO.

## 2. Surfactants in PPy NPNT structure after synthesizing

After the polymerization, the AAO with PPy-NPNT was immersed in absolute ethanol at 60 °C for 1 day to remove residual surfactants which should be embedded in PPy NPNT structure. Additional step for removing residuals and surfactant were also performed by ethanol filtration into the nanotube using cartridge method. The Thermogravimetric analysis (TGA) was used for verifying the P123 extraction. The TGA curve of the as-obtained AAO with PPy-NPNT showed a total loss of ca. 15 %. After washing step, however, the weight loss at between 100~300 °C was significantly reduced, and total weight loss also decreased to 9 %, indicating successful removal of surfactant from NPNT structure by ethanol treatment.

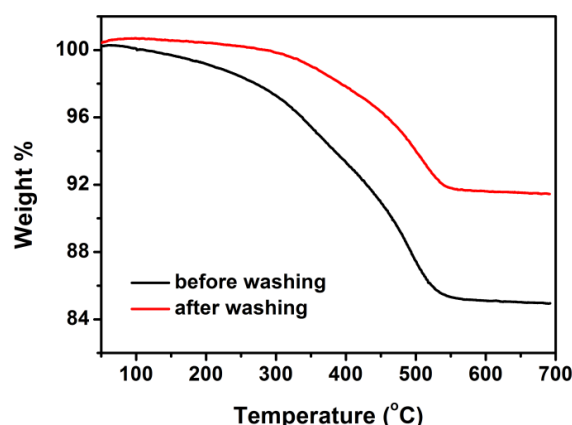


**Figure S1.** Thermogravimetric curves of before and after washing by ethanol filtration.

### 3. Polymerization mechanism of PPy

The vapour deposition polymerization can be accomplished by the oxidation of the pyrrole monomer in the same process as electrochemical polymerization, as following mechanism;

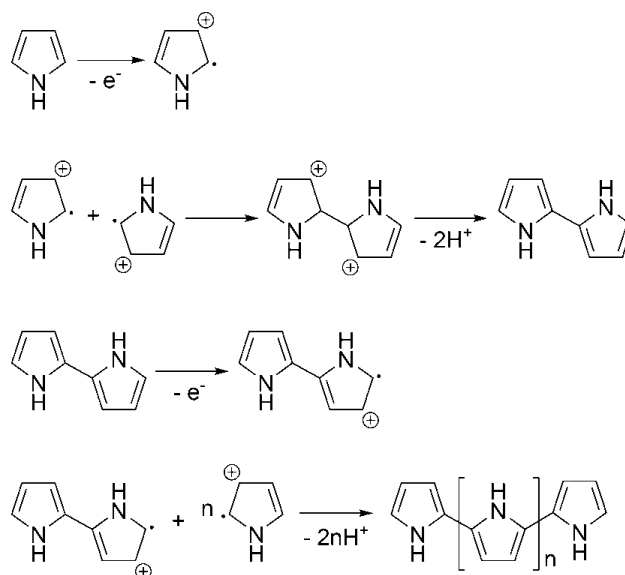


**Figure S2.** Polymerization mechanisms of pyrrole by oxidant.

The Fe cation has high oxidizing potential enough to make oxidized pyrrole monomer, and thus plays a role of initiator. Oxidized pyrrole monomer will be generated by Fe ions, and firstly, will form the dimer, as shown in Fig. S2. The activation energy for oxidation of dimer is generally lower than that of monomer, and thus propagations of polymerization will be easily occurred.

In the present work, we can control morphology of PPy NPNT structure by adjusting concentration of  $\text{FeCl}_3$  in surfactant solution. TEM images of PPy NPNT structure templated by P123 with the surfactant solution having different amount of  $\text{FeCl}_3$  are exhibited in Figure S3. The  $\text{FeCl}_3$  amount of Figure S1a was half of control experiment ( $\sim 0.05$  g in surfactant solution), and that of Figure S3c was 0.2 g. When the surfactant solution contained relatively small amount of oxidant, the nanoparticle with irregular morphology was observed inside AAO membrane and the particle population also decreases compared to Figure S3b. On the other hand, more robust particle structure is observed as increasing the amount of initiator. It could be concluded that the Fe cation is preferentially adsorbed on the wall of AAO owing to their electrostatic attraction, and the residual Fe ion is located in the micellar network. Therefore, as increasing the amount of  $\text{FeCl}_3$ , the particle size is augmented and robust structure is constructed.

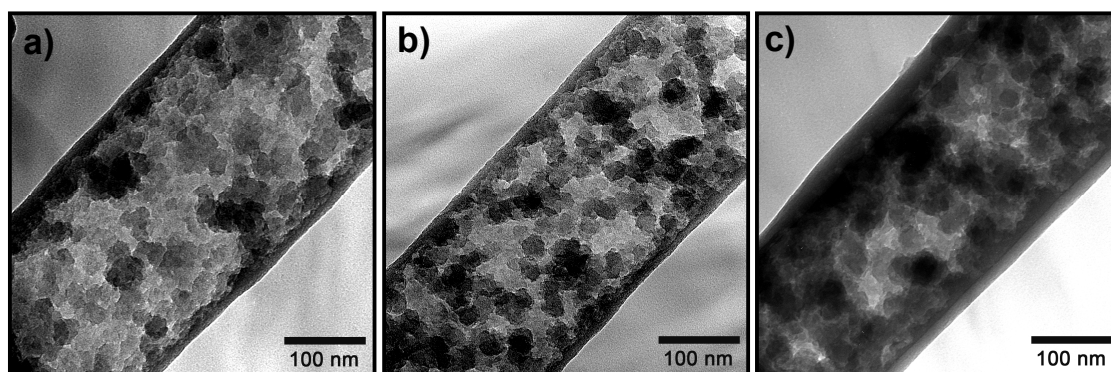


**Figure S3.** TEM images of PPy particle in nanotube structure fabricated from surfactant solution composed of a) 1 g of P123, 0.05 g of  $\text{FeCl}_3$ , 2 g of water and 5 g of ethanol b) 1 g of P123, 0.1 g of  $\text{FeCl}_3$ , 2 g of water and 5 g of ethanol (same image with Figure 2c), and c) 1 g of P123, 0.2 g of  $\text{FeCl}_3$ , 2 g of water and 5 g of ethanol.

#### 4. Control experimental; without ethanol in surfactant solution

To investigate the effect of solvent in the surfactant solution for NPNT formation, P123 surfactant was dissolved in water containing  $\text{FeCl}_3$  without ethanol. The dense structure of PPy NPNT (Fig. 2c) could not be obtained at this condition without ethanol. It is considered that evaporation of ethanol have essential contribution to form the micellar structure. With ethanol, the solution has dried gradually from the pore of AAO at 80 °C during VDP, and the ethanol will act as a heat reservoir, which make it possible to maintain their micellar structure during evaporation. So the optimum condition for NPNT was fixed to 1 g of P123, 2 g of water, 5 g of ethanol, 0.1  $\text{FeCl}_3$ , after wide range of trial.

#### 5. Temperature control.

The PPy NPNT structures were also fabricated at different reaction condition. Because the boiling point of pyrrole monomer is about 131 °C, relatively weak electron density is observed, when the VDP is performed at 60 °C (Figure S4a). The particle sizes in nanotubes are also smaller than that of NPNT prepared in high-temperature, mainly due to lack of pyrrole monomer and corresponding weak vapor pressure. On the other hand, when the VDP is carried out in 120 °C (Figure S4c), the nanotubes contained densely packed nanoparticles. In addition, the particle size is about 40 nm, which is larger than that of NPNT prepared in 80 °C (Figure S4b).

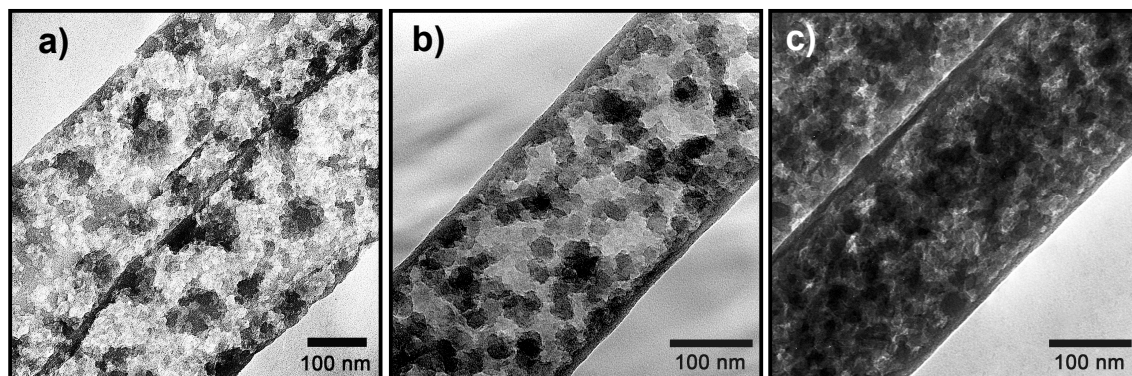


**Figure S4.** TEM images of PPy particle in nanotube structure fabricated from surfactant solution composed of 1 g of P123, 0.05 g of  $\text{FeCl}_3$ , 2 g of water and 5 g of ethanol in terms of different reaction temperature a) 60 °C, b) 80 °C (control; same with Figure 2c) and c) 120 °C

#### **6. PPy NPNT prepared by different type of soft-template (block-copolymer): Variation with Pluronic surfactant**

In the previous work, the mesoporous silica or carbon nanofibers had been obtained in the AAO-Pluronic block copolymer system. However, in the case of PPy VDP with Pluronic P series, PPy nanoparticles were located inside the nanotubes, instead of mesoporous species. As presented in Fig. S5, all of P series-block copolymer (P65, P84, and P103) could form NPNT structure with PPy particles of similar diameter. These P series has comparable chain length of ethylene oxide (EO) with various chain lengths of propylene oxide (PO). Accordingly, it could be concluded that the PPy nanoparticles were generated in the region of self-assembled PEO chain, as demonstrated in Scheme 1.

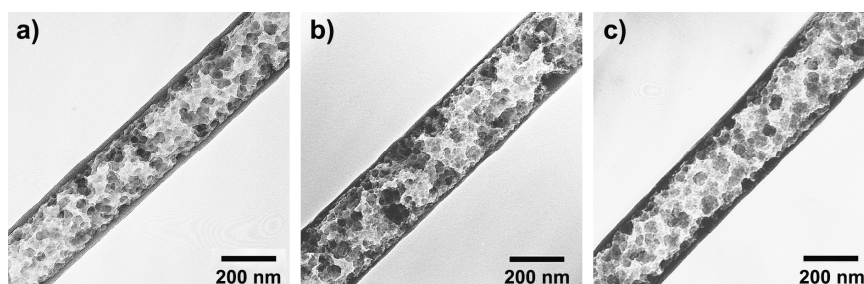


**Figure S5.** TEM images of PPy NPNT produced from a) P103, b) P84, and P65 solution.

## 7. Heavy metal ion removal by AAO membrane containing PPy nanotube and NPNT.

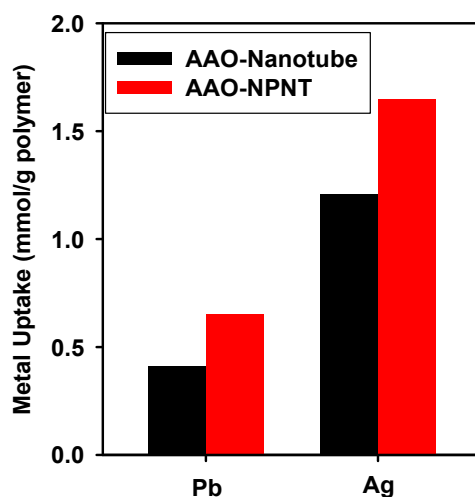


**Figure S6.** Heavy metal ion uptake by AAO membrane containing NT and NPNT

The adsorption property of heavy metal ions was evaluated by filtration method using the cartridge system in order to show advantages of NPNT structure over simple nanotube. The AAO membrane treated with PPy could be considered a membrane for removing heavy metal ions, owing to the nitrogen binding site of the PPy and their high surface area. The adsorption property was conducted as a function of the PPy nanostructure. AAO membrane containing PPy nanotubes shows comparable metal uptake amount with our previous works (ref S2). On the other hand, the NPNT structure exhibited enhanced adsorption property according to its high surface area (Figure S6). These results could provide new possibilities for maximizing the surface area of inside nanotubes.

Detailed experimental procedure for heavy metal ion adsorption is provided below and also in our previous work (ref S2);

The adsorption property of heavy metal ions was evaluated using AAO membrane containing different PPy nanostructures. The heavy metal ion solutions for  $\text{Pb}^{2+}$  and  $\text{Ag}^+$  ion were provided by dissolving lead nitrate ( $\text{Pb}(\text{NO}_3)_2$ ) and silver nitrate ( $\text{AgNO}_3$ ) in water with specific initial concentration (100 ppm), respectively. All of the solutions were sterilized by filtration with 0.20  $\mu\text{m}$  membrane filters. For adjusting pH value of the solutions to 6, nitric acid and ammonia solution were used.

The 10 mL of each heavy metal ion solutions were passed through the PPy NPNT/AAO membrane in the cartridge system at room temperature to investigate the uptake amount of the metal ions. The flow rate was fixed to 2 ml/h. And the uptake amount was calculated by measuring the residual metal ion after the

filtration, according to the following equations.

$$Q = \frac{(C_0 - C_e) \times V}{W} \quad (1)$$

where  $Q$  is the uptake amount of heavy metal ion in mmol (metal ion)/g (polymer),  $C_0$  and  $C_e$  is the initial concentration of metal ion solution and the equilibrium concentration of metal ions after removal experiment in mmol/L,  $V$  is the volume of metal ions solution in liter, and  $W$  is the weight of the adsorbent in gram scale.

Ref S2) M. Choi, and J. Jang, *J. Colloid Interface Sci.*, 2008, **325**, 287; J. Song, H. Oh, H. Kong, and J. Jang, *J. Hazard. Mater.*, 2011, **187**, 311.

## 8. Cartridge system details.

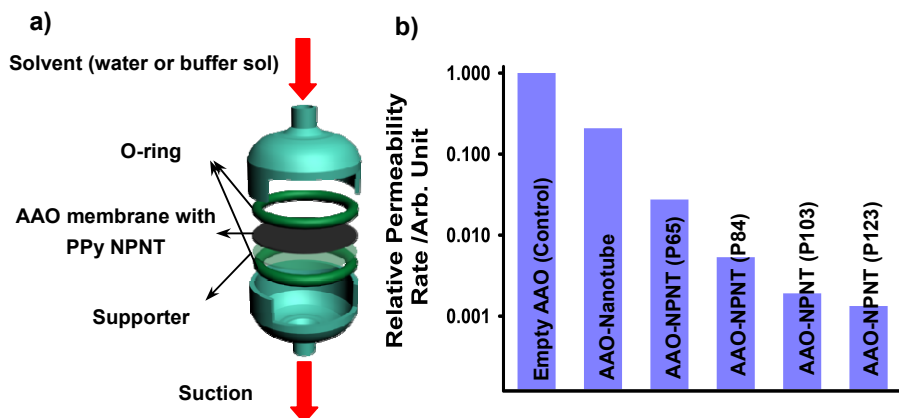


**Figure S7.** a) Schematic illustration of experimental setup to immobilize protein inside the pore of AAO and b) relative permeability of water through the AAO-NPNT membrane with respect to kinds of Pluronic block-copolymer.

Overall immobilization processes (washing with buffer, treatment of N-ethyl-N'-(3-dimethylaminopropyl)carbodiimide hydrochloride (EDC) and N-hydroxysuccinimide (NHS), and conjugation of Streptavidin or biotin) were performed in the cartridge system with vacuum suction, as drawn in Figure S7a. This could be more advantageous than the solution treatment, because the filtration method permitted specific immobilization of target compound in the pore of membrane (no binding on the surface of membrane or outside of nanotubes). The AAO-NPNT could be beneficial in this filtration system compared to the AAO-nanotube, due to the retardation of flow rate and high surface area for

binding site.

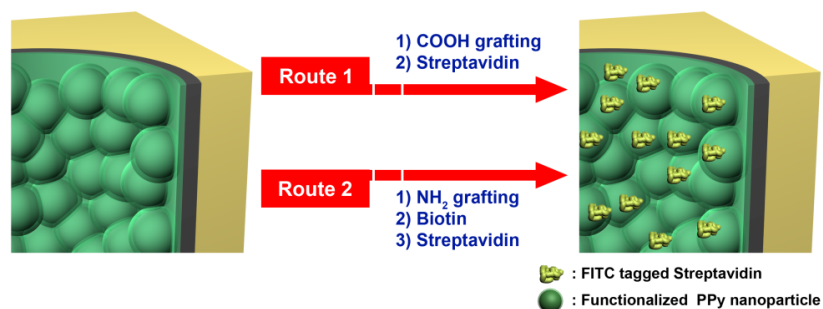
The AAO-NPNT membrane was located in the cartridge as shown in Figure S6a to measure water permeability of functionalized AAO. The AAO membrane containing PPy NPNT is supported by mesh membrane to endure the pressure endowed, and Teflon O-ring is inserted to prevent possible leakage. The relative permeability of water through the AAO-NPNT membrane was measured using vacuum suction, as a function of corresponding block copolymer kinds. Relative permeability rate ( $R_{p,rel}$ ) is defined as following;

$$R_{p,rel} = t / t_{empty} \quad (1)$$

, where  $t$  is the required permeation time for certain amount of water through each sample and  $t_{empty}$  means the required permeation time through empty AAO. The relative permeable rate of each AAO-NPNT membrane with respect to that of empty AAO is represented in Figure S7b. It is obvious that the permeable rate decreased when the nanotubes contain the nanoparticles. Furthermore, the permeable rate of AAO-NPNT membrane is slower than that of AAO-nanotube membrane, because the particles in nanotube could play a role in bead for reducing the flow rate. It is noteworthy that the average permeable rate is different when the block copolymers are altered in fabrication procedure. The AAO-NPNT membrane from P65 has the highest flow rate, whereas that from P123 reaches the lowest flow rate. Although particles in each NPNT structure has similar diameter at TEM observation, it could be expected that there must be some discrepancy in network formation. The relative permeability is reduced with increasing molecular weight of the block copolymer. In the case of high molecular weight, the self-assembled structure should prefer forming the micellar network to the isolated micelles. Brunauer-Emmett-Teller (BET) surface areas of each PPy NPNT produced from P123, P103, P84 and P65 are estimated as 48, 45, 40, and 34  $m^2 g^{-1}$  (measured after AAO removal), respectively, indicating that the NPNT structures with densely-packed nanoparticles are constructed from block copolymer with high molecular weight.

## 9. Two different strategies to immobilize protein.

Two different methods were applied to immobilize a protein in the pore of AAO, as denoted in Scheme S1. Firstly, the FITC-Streptavidin was directly immobilized on the carboxyl functional groups of PPy NPNT (route 1). For that, After washing the membrane with phosphate buffered saline (PBS), FITC-Streptavidin was anchored on the surface of COOH-NPNT by aid of EDC + NHS in buffer solution. Secondly, N-amino-pyrrole ( $NH_2$ -Py) was firstly grafted and biotin was treated. FITC-Streptavidin was consecutively conjugated on the biotinlated-NPNT (route 2). In the both cases, the membrane was washed several times with the PBS to remove residual Streptavidin.



**Scheme S1.** Scheme of Streptavidin immobilization onto the functionalized-nanoparticles in the PPy NPNT.

The FTIR spectrum of COOH-NPNT treated with NHS ester is also presented in Figure S8. The characteristic peaks of NHS such as peak at  $1780\text{ cm}^{-1}$  which could be assigned to NHS ester are observed, as well as the all of characteristic peaks of COOH-NPNT.

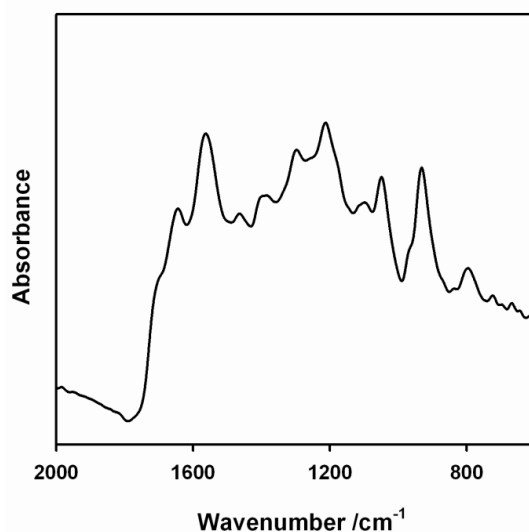


**Figure S8.** FTIR spectra of PPy NPNT grafted by functional monomer (COOH-Py) after modifying with NHS

#### 10. Comparison of absorption amount on COOH-NPNT and NH<sub>2</sub>-NPNT membrane and lowest detectable concentration of Streptavidin.

Population of emission site for the two different functionalized PPy NPNT membranes was calculated using imageJ<sup>TM</sup> for the quantitative comparison. Threshold process was applied to the Fig. 4 in order to

calculate the accurate emission area for the FITC-Streptavidin. The emission area of NH<sub>2</sub>-NPNT membrane (64.64 %) was approximately four-and-a-half times larger than that of COOH-NPNT membrane (14.11 %).

Lowest concentration of Streptavidin which is detectable with identical experimental procedure was determined as 0.1 mg/mL. At the 0.1 mg/mL concentration of Streptavidin, similar emission site with that of Figure 4 was detected. However, it is hard to conclude that Streptavidin is successfully immobilized on the membrane at lower concentration than Streptavidin concentration of 0.1 mg/mL.